PERSPECTIVE

The rich physics of A-site-ordered quadruple perovskite manganites AMn_7O_{12}

Alexei A. Belik, [iD] *[a] Roger D. Johnson [iD] [b] and Dmitry D. Khalyavin [iD] [c]

Perovskite-structure $AMnO_3$ manganites played an important role in the development of numerous physical concepts such as double exchange, small polarons, electron–phonon coupling, and Jahn–Teller effects, and they host a variety of important properties such as colossal magnetoresistance and spin-induced ferroelectric polarization (multiferroicity). A-site-ordered quadruple perovskite manganites AMn_7O_{12} were discovered shortly after, but at that time their exploration was quite limited. Significant progress in their understanding has been reached in recent years after the wider use of high-pressure synthesis techniques needed to prepare such materials. Here we review this progress, and show that the AMn_7O_{12} compounds host rich physics beyond the canonical $AMnO_3$ materials.

1. Introduction

Perovskite-structure manganites have experienced waves of intensive study,[1] starting in the late 1940s with the discovery of conductive and ferromagnetic (FM) properties and metal–insulator transitions in mixed-valence $R_{1-x}A_xMnO_3$ (R = trivalent cations and A = divalent cations). A theoretical understanding of these properties was quickly developed, including the theory of double exchange[2] and Goodenough's one-electron electronic structures.[3] Then followed the discovery of colossal magnetoresistance (CMR),[4] prompting intensive work on single crystals and thin films, and the proposal of magnetic and electronic phase separation scenarios.[5] Perovskite manganites also played an important role in the revival of interest in multiferroic and magnetodielectric materials with $RMnO_3$ (R = Tb and Gd) hosting some of the largest values of spin-induced ferroelectric polarization.[6] They were also intensively studied as catalysts,[7] solid mixed-conductive electrolytes, electrode materials, thermoelectric ceramics and sensors. This remarkable diversity in physical properties is rooted in considerable structural and chemical flexibility. As such, the perovskite manganites have become canonical systems for the study of structure–property relationships in strongly correlated electron systems.

[a]*International Center for Materials Nanoarchitectonics (WPI-MANA), National Institute for Materials Science (NIMS), Namiki 1-1, Tsukuba, Ibaraki 305-0044, Japan. E-mail: Alexei.Belik@nims.go.jp*

[b]*Department of Physics and Astronomy, University College London, Gower Street, London, WC1E 6BT, UK*

[c]*ISIS Facility, Rutherford Appleton Laboratory, Chilton, Didcot, OX11 0QX, UK*

Alexei A. Belik is a principal investigator at the National Institute for Materials Science (NIMS), Japan, which he jointed as a permanent member in 2006. He holds a PhD in Inorganic Chemistry from Moscow State University, Russia. He was a postdoctoral researcher at NIMS (2000–2002 and 2004–2006) and Kyoto University, Japan (2002–2004). His current interests are in high-pressure synthesis of new materials (mainly oxide perovskites) and their characterization.

Alexei A. Belik

Roger Johnson is a lecturer in condensed matter physics at University College London and a Royal Society University Research Fellow. He works in the area of quantum materials and physical crystallography. Crystal and magnetic structure solutions are obtained by multiple diffraction-based methods, and combined with symmetry analysis by group and representation theory, Roger determines structure–property relationships in inorganic oxides, halides, and hybrid organic–inorganic materials.
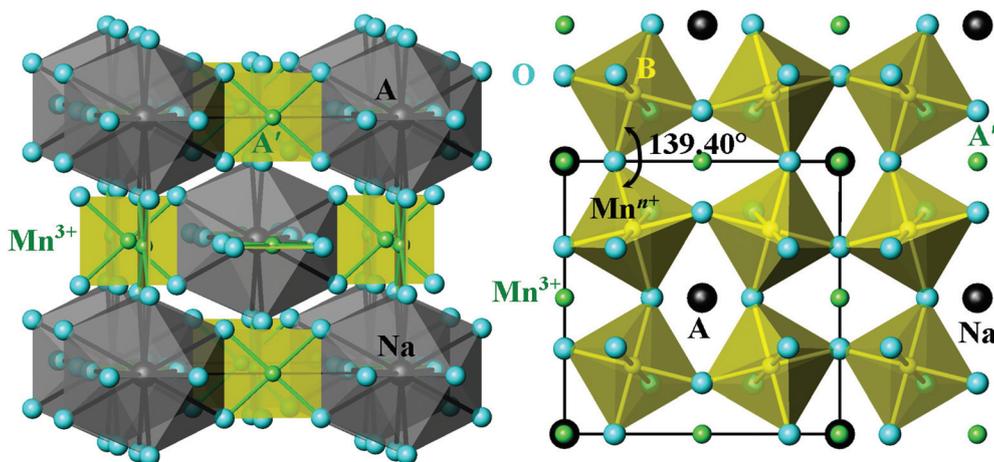
Roger D. Johnson

Fig. 1 Crystal structure of the parent cubic modification of A-site-ordered quadruple perovskites AMn_7O_{12} and $AA'_3B_4O_{12}$ in space group $Im\bar{3}$ exemplified by the structure of $NaMn_7O_{12}$ at RT.[12] An Mn−O−Mn (B−O−B) angle is given. A-site polyhedra are shown on the left, and B-site octahedra — on the right.

AMn_7O_{12} manganites (with A = Na, divalent and trivalent cations) are a special subfamily of perovskite-type materials, namely the A-site-ordered quadruple perovskites[8] with general chemical formula $AA'_3B_4O_{12}$. Three quarters of large A cations are replaced by small Mn^{3+} cations at the A′ sites with an effective square-planar coordination (Fig. 1). By heterovalent substitution of the A cations, which have a large 12-fold coordination (Fig. 1), one can obtain mixed-valence states of Mn at the B sites, *i.e.* $A^{n+}Mn^{3+}_3(Mn^{3+}_{1+n}Mn^{4+}_{3-n})O_{12}$, in close analogy to $R_{1-x}A_xMnO_3$. The AMn_7O_{12} compounds are stabilized by very large tilts of the $a^+a^+a^+$ type in Glazer's notation,[9] requiring high-pressure high-temperature treatments for their preparation (except for $CaMn_7O_{12}$, which can be synthesised at ambient pressure). Such an 'exotic' synthesis procedure could be the main reason why they did not attract much attention immediately after their discovery despite great interest in the classical mixed-valence $R_{1-x}A_xMnO_3$ perovskites. Only with the widespread use of high-pressure facilities has research on AMn_7O_{12} intensified, and significant progress in their under-

standing has been reached in recent years. In this work, we review the recent progress on AMn_7O_{12} manganites.

Because of the space limitations we cannot cite all references, especially those devoted to $CaMn_7O_{12}$. Therefore, only foundational references are given that are widely cited in latter works.

2. NaMn₇O₁₂

$NaMn_7O_{12}$ was the first compound of the AMn_7O_{12} series to be discovered (in 1973) and was found to crystallize in an $Im\bar{3}$ cubic structure at room temperature (RT) (Fig. 1); now identified as the parent aristotype to all AMn_7O_{12}.[10] A low-temperature (LT) structural phase transition near T_{CO} = 176–190 K (CO stands for charge order) was soon found (Fig. 2), below which a monoclinic $I2/m$ crystal symmetry with $1Mn^{3+}:1Mn^{4+}$ B site charge order was suggested (here, the pattern of charge ordering is analogous to the pattern of orbital ordering associated with the $I2/m$ structure of $LaMn_7O_{12}$ (see part 4)).[11] Despite clear parallels with the widely studied half-doped $R_{0.5}A_{0.5}MnO_3$ perovskite manganites also containing a $1Mn^{3+}:1Mn^{4+}$ mixture at the B sites, $NaMn_7O_{12}$ attracted little attention for nearly 30 years.

Magnetic studies were performed in 2004, which showed two magnetic transitions at T_{N1} = 125 K and T_{N2} = 92 K.[12] It was suggested that Mn magnetic moments at the B sites order first at 125 K with an AFM-CE-type structure (AFM stands for antiferromagnetic), which can be described by two propagation vectors; k = (1/2, 0, −1/2) and k = (0, 0, 0). Mn moments at the A′ sites were reported to order at 92 K with an anti-body-centered arrangements of spins with propagation vector k = (0, 1, 0).[12] In this study the symmetry of the LT phase was taken to be $I2/m$ (see above) with compressed Jahn–Teller (JT) distortions of the Mn^{3+} B sites. However, a theoretical study in 2014 pointed out inconsistencies between the reported experimental
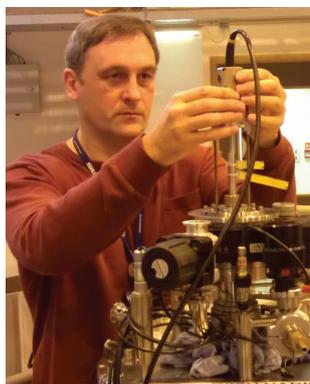
Dmitry D. Khalyavin is an instrument scientist at the ISIS Facility of the Rutherford Appleton Laboratory. He runs the high-resolution cold-neutron diffractometer WISH primarily designed for powder and single crystal diffraction in magnetic and large unit cell systems. The main Dmitry's expertise is magnetic crystallography, structural and magnetic phase transitions as well as diffraction methods in solid state physics.
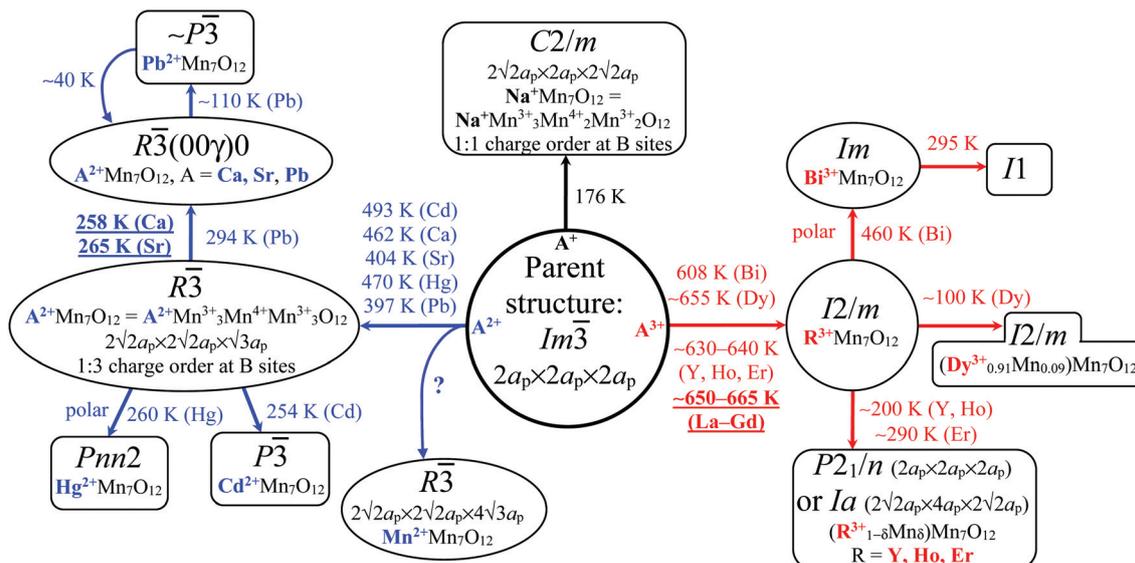
Dmitry D. Khalyavin

Fig. 2 A diagram of temperature-driven structural distortions in AMn_7O_{12} manganites from the parent cubic structure. Transition temperatures are reported on the figure when available. All distortions keep the $2a_p \times 2a_p \times 2a_p$ cell (with $\alpha \approx \beta \approx \gamma \approx 90°$) except trigonal systems (with $\alpha = \beta = 90°$ and $\gamma = 120°$), $C2/m$ (ref. 13 and 14; with $\alpha = \gamma = 90°$ and $\beta \approx 90°$) and Ia (ref. 68; with $\alpha = \gamma = 90°$ and $\beta \approx 90°$). Note that for the $R\bar{3}$ distortion with $2\sqrt{2}a_p \times 2\sqrt{2}a_p \times \sqrt{3}a_p$, the $2a_p \times 2a_p \times 2a_p$ cell (with $\alpha = \beta = \gamma \approx 90°$) can also be constructed (using rhombohedral axes and non-standard setting). For $MnMn_7O_{12}$, a $4a_p \times 4a_p \times 4a_p$ cell with $F\bar{1}$ symmetry was also reported at RT.[37] $a_p \approx 3.8$ Å is a lattice parameter of the cubic ABO_3 perovskite (space group $Pm\bar{3}m$). For underlined compositions there are no further structural transitions.

crystal and magnetic structures.[13] The theoretical work[13] proposed an alternative LT crystal structure, which was soon confirmed experimentally.[14] This correct LT structure has $C2/m$ symmetry, a $2\sqrt{2}a_p \times 2a_p \times 2\sqrt{2}a_p$ superstructure with $\alpha = \gamma = 90°$ and $\beta \approx 90°$ (where a_p is a lattice parameter of an ideal cubic ABO_3 perovskite), full static Mn^{3+}/Mn^{4+} charge ordering, and elongated JT distortions of the Mn^{3+} B sites. This LT crystal structure can be described in terms of a commensurate modulation of the parent cubic structure with propagation vector $\mathbf{k} = (1/2, 0, -1/2)$. Importantly, this structural modulation is consistent with the magnetic propagation vectors observed below 125 K.

We believe that the magnetic structures of $NaMn_7O_{12}$ need re-investigation considering recent results on the magnetic structures of all other AMn_7O_{12} and RMn_7O_{12} manganites (see parts 3 and 4), where simultaneous ordering of Mn at the B and A′ sites was observed. An additional magnetic anomaly near 34 K was recently reported in $NaMn_7O_{12}$,[15] which, in our opinion likely originates in an impurity: $MnCO_3$ has a magnetic transition with weak FM-like properties at this temperature, and an X-ray diffraction pattern reported in (ref. 16) gave evidence for the presence of an $MnCO_3$ impurity (a 100% peak of $MnCO_3$ near 31.5° was observed; note that (ref. 16) incorrectly assigned impurity peaks).

$NaMn_7O_{12}$ is a weak insulator with thermally activated charge transport, and resistivity increases by about one order of magnitude below T_{CO}.[12] $NaMn_7O_{12}$ ceramics also showed dielectric anomalies at T_{CO} and additional relatively sharp step-like frequency-dependent dielectric anomalies from 50 K (at $f = 1$ kHz) to 80 K (at $f = 1$ MHz).[15,17] These steps were orig-

inally left without explanation.[17] Similar step-like dielectric behavior was observed in RMn_7O_{12} (R = La, Ce, Sm, Eu and Gd) between 17 and 35 K, which was assigned to extrinsic effects (see part 4). No apparent dielectric anomalies were detected in $NaMn_7O_{12}$ at T_{N1} and T_{N2}.[17] Broad and symmetrical pyroelectric current anomalies were observed in $NaMn_7O_{12}$ from 20 K to 40 K, which were assigned to a (spin-induced) ferroelectric transition associated with the 34 K magnetic anomaly.[15] Following the results of more recent detailed studies of other AMn_7O_{12} compounds (see part 4), we expect that the dielectric and pyroelectric current anomalies in $NaMn_7O_{12}$ are most probably caused by extrinsic effects.

A number of works were devoted to the single-crystal growth of $NaMn_7O_{12}$.[16,18] It was found that small amounts of water and Na excess facilitate the crystal growth. The formation of good samples was observed in the pressure range of 2–6 GPa and temperature range of 670–1120 K with the best conditions at 6 GPa and 1100 K. Single-crystal X-ray diffraction studies gave the real chemical composition of the studied crystal as $(Na_{0.95}Mn_{0.05})Mn_7O_{12}$.[16] No structural phase transitions were found up to 40 GPa (at RT), but some anomalies in resistivity near 18 GPa gave evidence for charge transfer from the B site to the A′ site.[19]

3. AMn_7O_{12} (A = Mn, Cd, Ca, Sr, Hg and Pb)

Perovskites with A = Ca, Cd and Sr were first reported by Bochu *et al.*[20] and synthesized under high-pressure and high-

temperature (HT) conditions. Later, Horowitz and Longo[21] prepared powder samples of $CaMn_7O_{12}$ at ambient pressure and so far this is the only member whose synthesis does not require extreme conditions. The authors also pointed out the mixed-valence character of this oxide. The charge degree of freedom has been found to be mainly localized on the B-site Mn ions, resulting in 3 : 1 charge order between Mn^{3+} and Mn^{4+} in the RT trigonal structure with $R\bar{3}$ symmetry and apically compressed $Mn^{3+}O_6$ octahedra.[22] The latter implies that, unlike the vast majority of known JT systems with two longer and four shorter Mn–O distances (JT elongation), the $Mn^{3+}O_6$ octahedra in $CaMn_7O_{12}$ are characterized by four longer and two shorter Mn–O distances (JT contraction, Fig. 3a). Hence, it was suggested that this perovskite represented a new type of JT distortion of Mn^{3+} cations in oxides, with x^2–y^2-type orbital ordering.[22] This is a very unusual situation because the occupation of x^2–y^2 orbitals of Mn^{3+} with locally compressed octa-

hedra has been shown by Khomskii and van den Brink to be unstable due to anharmonic effects which always stabilize elongated octahedra.[23] The transition to the trigonal charge-ordered phase takes place well above RT and is associated with phase coexistence in the temperature range of 409–448 K where the LT trigonal phase coexists with the HT cubic one.[24] The LT structural studies[25–28] revealed another transition at $T_{OO} = 260$ K (OO stands for orbital order), where the crystal structure of $CaMn_7O_{12}$ develops an incommensurate structural modulation with propagation vector $k_S = (0, 0, \gamma)$ ($\gamma = 0.9215$ at $T = 113$ K,[29] in the following discussion we will use the equivalent propagation vector $(0, 0, 3) - k_S = (0, 0, 2.0785)$ to emphasize its relation with the modulation of the magnetic order). Initially, the modulation was assigned to charge ordering,[25] however, subsequent quantitative structure refinement of synchrotron X-ray and neutron powder diffraction data in the $R\bar{3}(0,0,\gamma)0$ superspace group[27] did not support this
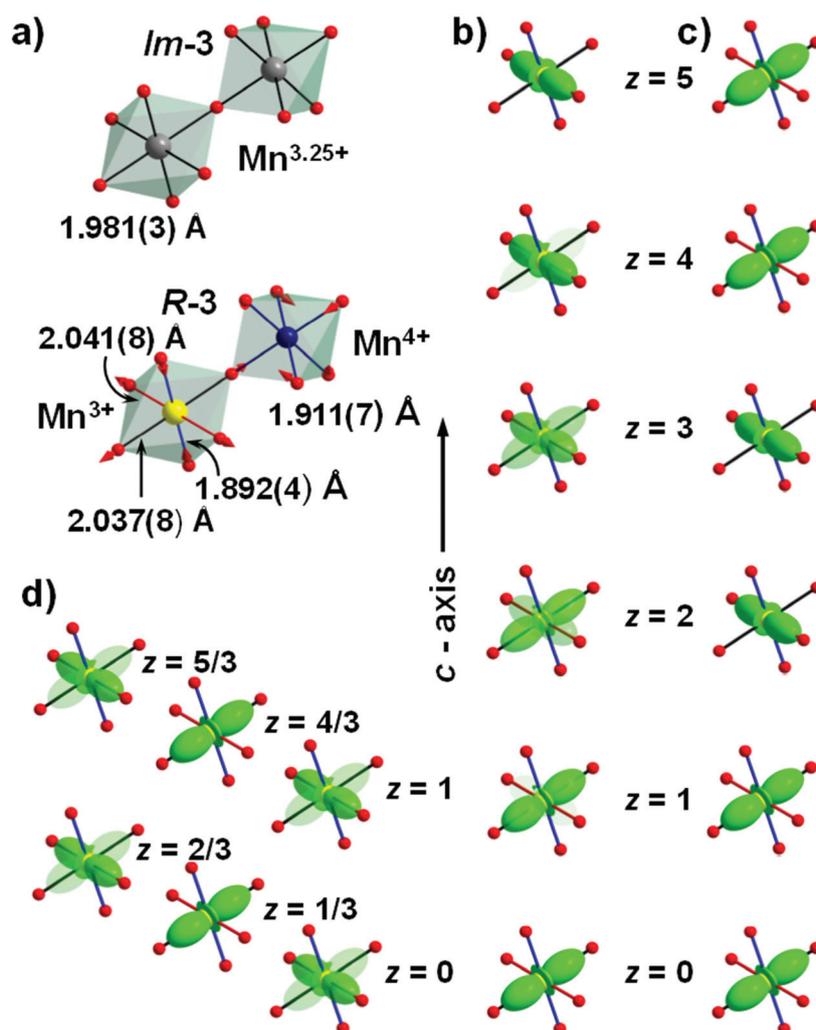

Fig. 3 (a) Compression of $Mn^{3+}O_6$ octahedra in $CaMn_7O_{12}$ at the phase transition from the disordered cubic $Im\bar{3}$ to the charge-ordered trigonal structure (Mn−O bond distances are taken from ref. 24 and 22 for the cubic and trigonal structures, respectively). Orbital density wave in $CaMn_7O_{12}$ (b), ξ-Mn_2O_3 (c) and $CdMn_7O_{12}$ (d), illustrating the change of orbital state of Mn^{3+} upon propagation along the trigonal axis. In the latter case, the commensurate orbital density wave splits the Mn position into two sites with fully and partially polarised states.

interpretation and instead revealed a complex modulation of Mn–O bond distances. The model was confirmed by Perks *et al.*[30] using X-ray single-crystal data, and the modulation was interpreted as an incommensurate orbital ordering (orbital density wave) localised on the B-site Mn^{3+} cations. The density wave implies a periodic change of the $3x^2–r^2$ and $3y^2–r^2$ orbital occupancies passing through the $x^2–y^2$ state only at the nodal points (Fig. 3b). In other words, in the modulated structure most of the octahedra are locally elongated along one of two axes that alternate periodically within the crystal, giving rise to the apical compression of octahedra on average.

The systematic structural study by Belik *et al.*[29] revealed a similar modulation in other members of the family with A = Sr, Cd and Pb, taking place at T_{OO} = 265 K, 254 K and 294 K, respectively (Fig. 2). The propagation vector for the Sr-perovskite is also incommensurate with the magnitude very close to the Ca-counterpart; k_S = (0, 0, 2.0765) at T = 113 K. The modulation was found to be commensurate, k_S = (0, 0, 2), in the case of $CdMn_7O_{12}$, giving rise to the primitive unit cell with $P\bar{3}$ symmetry. The commensurate nature of the orbital density wave was interpreted as an activation of a third-power lock-in term allowed in the Landau free-energy decomposition when the γ-component of the propagation vector takes the commensurate value.[31] The centrosymmetric space group fixes the global phase of the commensurate orbital density wave and imposes a stacking of fully and partially polarized orbital states (Fig. 3d).

Note that some samples of $CdMn_7O_{12}$ showed phase separation below about 60 K,[31,32] characterised by a mixture of $P\bar{3}$ and $I2/m$ phases and large hysteresis in properties.[33] This coexistence likely reflects small variations in the real chemical compositions of such samples, and the appearance of the $I2/m$ phase needs detailed investigations as it usually appears in $R^{3+}Mn_7O_{12}$ (Fig. 2).

The situation with $PbMn_7O_{12}$ has been found to be more complicated.[34] Just below the transition at T_{OO} = 294 K the modulation is incommensurate with γ ~2.08. At T_{OO2} = 110 K another structural transition takes place where the propagation vector suddenly drops down to a quasicommensurate value k_S = (0, 0, 2.0060(6)). The quasicommensurate phase is stable in the temperature range of 40–110 K, and below T_{OO3} = 40 K the propagation vector jumps back to the incommensurate value k_S = (0, 0, 2.060(6)). Both the LT structural transitions are strongly first order with large thermal hysteresis. The orbital density wave in the quasicommensurate phase has been found to be substantially suppressed in comparison with the incommensurate phases, and this behaviour was attributed to a competition between the Pb^{2+} lone electron pair and Mn^{3+} JT instabilities. This makes this perovskite particularly attractive as a new playground for various charge doping strategies by analogy with the $BiMn_7O_{12}$ system (see section 5, below), where a light hole doping has been shown to stabilize exotic electric dipole and orbital textures due to a fine tuning of the relative strength of these two electronic instabilities.[35] Similar to $CaMn_7O_{12}$, the perovskites with A = Sr, Cd and Pb exhibit a HT transition to the cubic $Im\bar{3}$ structure at T_{CO} = 404 K, 493 K

and 397 K, respectively, as determined by differential scanning calorimetry.[33] We note that in other studies, T_{CO} for $PbMn_7O_{12}$ was reported to be 380 K,[36] and for $CaMn_7O_{12}$ prepared at high pressure – to be 462 K,[33] suggesting that T_{CO}, and also T_{OO}, are sensitive to the sample quality.

Another member of the $A^{2+}Mn_7O_{12}$ family is the ξ-polymorph of Mn_2O_3. As has been shown by Ovsyannikov *et al.*,[37] at high temperature (above 1000 K) and at high-pressure (above 18 GPa), Mn_2O_3 transforms to a perovskite modification which can be quenched into a metastable phase at ambient conditions. This metastable phase exhibits a unique charge disproportionation phenomenon stabilizing the quadruple perovskite structure $Mn^{2+}Mn^{3+}_3Mn^{3.25+}_4O_{12}$ with an additional $3Mn^{3+}:1Mn^{4+}$ charge ordering and commensurate orbital density wave with k_S = (0, 0, 9/4), localized in the B-site perovskite position. The charge ordered modulated structure possesses $R\bar{3}$ symmetry with a $2\sqrt{2}a_p \times 2\sqrt{2}a_p \times 4\sqrt{3}a_p$ supercell defined with respect to the pseudocubic simple perovskite structure which is prototype for all families of perovskite materials. Here, the orbital density wave represents a sequence of $3x^2–r^2$ and $3y^2–r^2$ orbital states ordered in a ++−− fashion (where + and − indicate distinct states) upon propagation along the trigonal axis (Fig. 3c). The commensurate nature of the orbital density wave and the associated structural modulation has been explained by a coupling of the orbital ordering to an independent structural distortion, which improves the poor bonding conditions of Mn^{2+} in the A-site perovskite position.[38] The trigonal structure has been reported to be stable at RT,[37] but the temperatures at which the B-site charge and orbital ordering onset are yet to be determined.

One more perovskite with a divalent A-site cation, $HgMn_7O_{12}$, has been recently reported by Chen *et al.*[39] Similar to other members of the family, it exhibits a cubic to trigonal structural transition due to the $3Mn^{3+}:1Mn^{4+}$ charge ordering in the B-site manganese position. The transition is first order and takes place *via* phase coexistence in the temperature range of 470–490 K. However, instead of the modulated trigonal ground state, the LT structure of $HgMn_7O_{12}$ to a good approximation is commensurate orthorhombic with the polar $Pnn2$ symmetry. The transition to the orthorhombic phase takes place at 240–260 K and is associated with a further charge disproportionation where 1/3 of Mn^{3+} in the A′ position become Mn^{2+}, giving rise to $1Mn^{2+}:2Mn^{3+}$ charge ordering in the A′ square planar position as well as $1Mn^{3+}:1Mn^{4+}$ charge and orbital ordering in the B-site position (Fig. 4). The polar symmetry is a result of the common action of two irreducible order parameters. One of them is the charge/orbital order and another serves to improve the coordination environment of the A′-site Mn^{2+} cations by making the environment more regular through shortening the second-nearest-neighbour distances. The charge transfer between the A′ and B sites has been suggested as an alternative mechanism to the orbital density wave formation to release the instability associated with the compressed octahedra in the 3 : 1 charge ordered trigonal phase. The B-site Mn^{3+} in this phase was assumed to exhibit orbital disorder between the $3x^2–r^2/3y^2–r^2$ states. Whether this
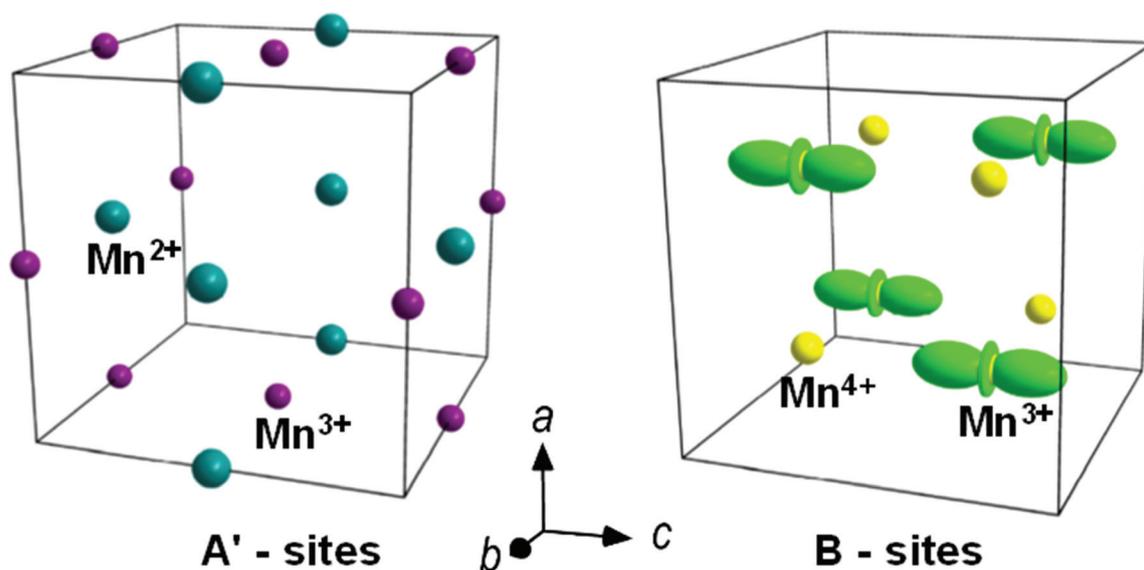
Fig. 4 Charge (left) and orbital (right) ordering in the orthorhombic $Pnn2$ phase of $HgMn_7O_{12}$ perovskite.[39]

is the case, or the x^2–y^2 orbital state is imposed by the bilinear coupling to the atomic displacement mode accompanying the 3 : 1 charge order[40] is an interesting open question.

The perovskites of the $A^{2+}Mn_7O_{12}$ family attracted great attention after the discovery of prominent multiferroic properties in $CaMn_7O_{12}$.[41,42] Long-range magnetic ordering in this material takes place at $T_{N1} \sim 90$ K with the incommensurate propagation vector, k_0, locked to the structural modulation such that $k_0 = k_S/2$.[26–28] Below $T_{N2} \sim 48$ K, the magnetic subsystem delocks from the structural modulation giving rise to a complex multi-k magnetic ground state.[43] The initially reported giant spin-driven polarization was found to onset at T_{N1}. Later studies[44] confirmed the multiferroic properties of $CaMn_7O_{12}$ but the electrical polarization was found only below the second magnetic transition at T_{N2} with substantially lower magnitude. The corresponding ground state magnetic structure was quantitatively determined using high-resolution neutron powder and single crystal diffraction data[43] and was found to represent an unprecedented example of helical order with modulated spin chirality (Fig. 5). Unlike usual helical structures with a constant magnetic phase between spins related by a lattice translation along the propagation vector, the magnetic phase of the spins in the ground state of $CaMn_7O_{12}$ is incommensurately modulated with the periodicity of the orbital density wave. The magnetic structure decomposes into a set of magnetic order parameters with distinct propagation vectors, $k_{n\pm}$, along the trigonal axis. A symmetry based phenomenological approach[43] revealed that this exotic ground state is a result of coupling between the primary magnetic order, stabilized by competing exchange interactions and referred to as the fundamental component $k_0 = (0, 0, 1.12354(8))$, and the orbital density wave $k_S = (0, 0, 2.0775(1))$ at $T = 1.5$ K (magneto-orbital coupling). By symmetry, the fundamental helical order alone cannot lock to the structural
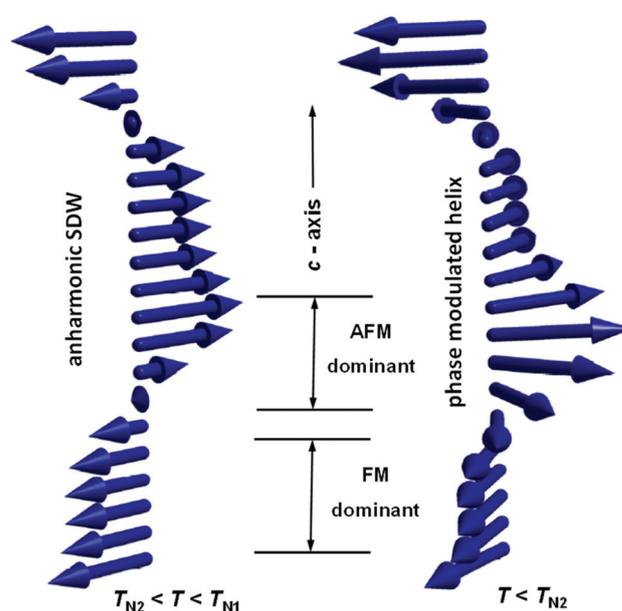

Fig. 5 Schematic representation of the anharmonic spin density wave (SDW) and the phase modulated helix, corresponding to the high-temperature lock-in phase and the ground state of $A^{2+}Mn_7O_{12}$ manganites.[43]

modulation, and hence the coupling introduces additional magnetic components with $k_{n\pm} = k_0 \pm nk_S$ propagation vectors. Experimentally, the components up to $n = 2$ have been confirmed.[43] Microscopically, the magneto-orbital coupling implies that the orbital density wave modulates the competing exchange interactions and local anisotropies resulting in faster and slower rotations of spins upon propagation along the trigonal axis.

The spin-driven electric polarization in $CaMn_7O_{12}$ has been explained by the ferroaxial mechanism[41] first proposed to explain multiferroic properties of $Cu_3Nb_2O_8$.[45] The mechanism describes a bi-linear coupling between spin chirality and polarization in crystals with axial distortions, known as ferroaxiality. The latter is a ferroic property like ferroelectricity and ferromagnetism, characterized by the presence of a well-defined rotation between different elements of the crystal structure (octahedral tilting in the given case). The trigonal crystal structure of $A^{2+}Mn_7O_{12}$ with point group $\bar{3}$ belongs to the ferroaxial class. The relevant microscopic interaction giving rise to the macroscopic polarization is antisymmetric Dzyaloshinskii–Moriya (DM) exchange. This exchange can gain energy by distorting the crystal structure and/or the electronic density in the presence of non collinear spins.[46] A discussion of the ferroaxiality and the polar distortions optimizing the antisymmetric exchange in $CaMn_7O_{12}$ can be found in the work by Perks et al.[30]

Unlike the helical order, a spin density wave can be locked to the structural modulation associated with the orbital density wave.[43] This type of ordering therefore is the prime candidate for the magnetic structure of $CaMn_7O_{12}$ in the temperature range of $T_{N2} < T < T_{N1}$, where the magnetic and structural modulations are commensurate with each other, holding the $k_0 = k_S/2$ ratio (Fig. 5). The magneto-orbital coupling is expected to yield additional magnetic components making the spin density wave anharmonic, which was confirmed experimentally through the observation of higher order satellites (in particular the $3k_0$ propagation vector).[27,43] It has to be pointed out that experimentally it is challenging to distinguish the spin-density wave with the spins confined within the (ab)-plane of the trigonal structure and the helical order. However, the commensurate relation between the magnetic and structural modulations and the absence of electrical polarization in the lock-in phase[44] strongly support the existence of a spin density wave above T_{N2}. Another argument in favour of this scenario comes from the precise magnetic structure determination in the ξ-polymorph of Mn_2O_3.[38,47] Similar to $CaMn_7O_{12}$, this perovskite also exhibits two magnetic transitions at $T_{N1} = 100$ K and $T_{N2} = 50$ K, and mutiferroic properties below T_{N2}. The HT magnetic phase has been found to be commensurate and locked to the structural modulation. The spins in this phase are polarized along the c-axis forming an anharmonic longitudinal spin density wave. The magnetic structure is only partially ordered and contains 1/4 of the A-site Mn^{2+} cations with zero ordered moment. Below T_{N2}, the magnetic propagation vector becomes incommensurate ($k_0 = (0, 0, 1.2439(3))$ at $T = 1.5$ K) and the magnetic structure turns into a phase modulated constant moment cycloid with only a small admixture of a helical component. Thus, the magnetic behaviour of $CaMn_7O_{12}$ and ξ-Mn_2O_3 is very similar apart from the different magnetic anisotropy which is an easy-plane type in the former case and easy axis (along the trigonal axis) in the latter. The longitudinal spin density wave can be unambiguously distinguished from any other solution and therefore the sequence paramagnetic – spin density wave – constant moment magnetic structure with rotating spins is a well-established experimental observation for this perovskite.

Magnetic structures of the perovskites with A = Sr and Cd are very similar to the Ca-counterparts.[31] For these materials T_{N1} is at 87 K and 88 K, respectively and the LT T_{N2} transition occurs at 63 K for A = Sr and 33 K for A = Cd. The magnetic propagation vector k_0 for the former is $(0, 0, 1.15427(6))$ and for the latter $(0, 0, 1.0682(1))$ at $T = 1.5$ K, indicating that the periodicity of the fundamental helical component depends on the radius of the A-site cation. The $PbMn_7O_{12}$ perovskite exhibits an additional intermediate magnetic phase[31,48] related to the fact that the magnetic ordering onsets within the quasi-commensurate structural phase with a substantially suppressed orbital density wave. Like in other manganites of this series, the magnetic propagation vector of $PbMn_7O_{12}$ is locked to the structural modulation just below $T_{N1} = 83$ K. The lock-in phase is stable only in a narrow temperature range and at $T_{N2} = 77$ K the magnetic propagation vector delocks from the structural modulation giving rise to the incommensurate helical order with only weakly modulated spin chirality. In an early study,[31] this weakly modulated intermediate magnetic phase was interpreted as an unmodulated single-k helix, where the magneto-orbital coupling is fully suppressed. However, the latest work[34] confirmed the presence of very weak magnetic components $k_{n\pm}$ indicating a finite magneto-orbital coupling. At $T_{OO3} = 40$ K, the re-entrant transition to the incommensurate structural phase takes place, re-establishing the orbital polarization which in turn triggers a strong magneto-orbital coupling in the ground state helical structure of $PbMn_7O_{12}$ with the periodicity of the fundamental magnetic component being $k_0 = (0, 0, 1.18410(8))$ at 1.5 K.

Thus, the magnetic properties of the divalent A-site quadruple perovskites reveal a universal interplay between magnetic and orbital degrees of freedom, leading to the concept of magneto-orbital coupling. In the HT ordered state the periodicities of the magnetic and orbital subsystems lock together via commensurate magneto-orbital coupling. On cooling, these periodicities delock, allowing the system to evolve towards a multi-k magnetic ground state in which incommensurate magneto-orbital coupling gives rise to a modulation of the spin helicity. The stability of the locked and delocked magnetic phases is controlled by the balance between the entropy term (promoting a partially ordered state at higher temperatures), lock-in term, and magnetic exchange interaction requiring a propagation vector different from the orbital modulation.[31,43] While T_{N1} remains approximately constant across the series (apart from ξ-Mn_2O_3 which has the additional A-site magnetic sublattice and therefore a noticeably higher T_{N1}), the periodicity of the ground state magnetic structure and the LT transition T_{N2} both monotonically increase with increasing A^{2+} ionic radius. The only member of the family whose magnetic properties might differ significantly from that described above is $HgMn_7O_{12}$. Although, the magnetic structure is yet to be reported for this perovskite, there is no reason to believe that it should obey the common scenario where the lock-in phase is followed by the delocked phase-modulated

ground state, imposed by the magneto-orbital coupling. Its crystal structure does not support the orbital density wave, adopting instead the alternative mechanism associated with the inter-site charge transfer that results in distinct charge and orbital patterns. Interplay between these electronic degrees of freedom with magnetism is therefore a very exciting topic for future studies.

Finally, let us mention the very recent X-ray resonant elastic scattering study of $CaMn_7O_{12}$,[49] where using polarization analysis it was found that the satellites with $\mathbf{k_0}$ propagation vector are not purely magnetic. The authors conclude that there is one more phase transition around 30 K, where the periodicity of the magnetic ground state locks to the second harmonic of the orbital modulation (a second lock-in phase). It is quite hard to understand this conclusion based on symmetry grounds because this would require a free-energy term linear in the magnetic order parameter components and quadratic in the orbital density wave which is forbidden by time reversal symmetry. As discussed above, the ground state of $CaMn_7O_{12}$ is the multi-k modulated helix which consists of a set of magnetic order parameters creating additional structural modulations through magneto-elastic coupling. The periodicities of these structural modulations are twice bigger than the periodicities of the corresponding magnetic components and they have distinct symmetries from the orbital density wave. For instance, if one takes the second harmonic of the $\mathbf{k_{1+}} = \mathbf{k_0} + \mathbf{k_S}$ ($\mathbf{k_0}$ and $\mathbf{k_S}$ are found to be (0, 0, 1.12) and (0, 0, 0.94), respectively for the studied crystal), it coincides with $\mathbf{k_0}$ and can be the origin of the observed charge-like contribution to the corresponding satellites. Since $\mathbf{k_{1+}}$ is not an independent order parameter, its second harmonic can also be expressed through a higher order coupling term using the $\mathbf{k_0}$ and $\mathbf{k_S}$ order parameters. In particular, the relevant term will be linear in respect of the magneto-elastic structural modulation and quadratic in respect of both $\mathbf{k_0}$ and $\mathbf{k_S}$, whose explicit form can be worked out using the information provided in (ref. 43). The presence of this structural modulation is a natural consequence of the magneto-elastic coupling and does not require a phase transition. Thus, the interesting results reported by Gautam *et al.*[49] need a further detailed study, with a particular attention to the observed splitting of the orbital modulation below T_{N2}.

As $CaMn_7O_{12}$ is often prepared at ambient pressure in air it may contain different impurities. Magnetic anomalies from impurities are sometimes erroneously attributed to additional magnetic transitions of the main $CaMn_7O_{12}$ phase, for example, a FM-like anomaly near 43 K from an Mn_3O_4 impurity.

4. RMn_7O_{12} (R = Y, La, Ce, Pr, Nd and Sm–Er)

Quadruple perovskite manganites with trivalent rare earth cations at the A site ($R^{3+}Mn_7O_{12}$) with R^{3+} = La,[7,20,50–61] Ce,[59,62] Pr,[63] Nd,[20,59] Sm,[59,64] Eu,[59,64] Gd,[64] Tb,[64] Dy,[65] and Y[66–68] (in

order of decreasing ionic radii) have been reported in the literature. The authors have also synthesised compounds with R^{3+} = Ho and Er, but the results are yet to be published. Compounds with R^{3+} = Tm–Lu appear to lie beyond the stability range of the AMn_7O_{12} structural framework (when prepared at 6–8 GPa) owing to their small ionic radii. Indeed, emergent dipolar-glass-like states have been observed in $DyMn_7O_{12}$ and YMn_7O_{12},[65,67] understood to arise from the underbonding of R^{3+} cations as the boundary of structural stability is approached (discussed in detail below).

Given the trivalency of the rare-earth cations, all manganese ions adopt a formal 3+ oxidation state in the stoichiometric charge balanced system. RMn_7O_{12} can be prepared in the stoichiometric composition for R^{3+} = La–Gd. However, they take $(R_{1-x}Mn_x)Mn_7O_{12}$ compositions for R^{3+} = Tb–Er, determined through (1) the synthesis of single-phase samples of corresponding compositions, (2) the neutron powder diffraction structural analysis of $(Dy_{0.91}Mn_{0.09})Mn_7O_{12}$ (ref. 65) and (3) the single-crystal X-ray diffraction structural analysis of $(Y_{1-x}Mn_x)Mn_7O_{12}$ (N.B. in this case, the structural analysis cannot distinguish between the $Y_{1-y}Mn_7O_{12}$ and $(Y_{1-x}Mn_x)Mn_7O_{12}$ models).[68] Therefore, manganese at the A sites could then take the 2+ oxidation state in $(R_{1-x}Mn_x)Mn_7O_{12}$. For simplicity, we will often use the RMn_7O_{12} chemical formula.

B site ions are predominantly Mn^{3+} and hence JT active. $LaMnO_3$-type[69] B site orbital order has been observed at RT in all RMn_7O_{12} compounds, which imposes $I2/m$ space group symmetry (N.B. $PrMn_7O_{12}$ was found to adopt both $I2/m$ (two variations with different degrees of monoclinic distortions) and $R\bar{3}$ structures at RT, with the phase fractions controllable by synthesis conditions).[63] The $I2/m$ orbital order can be understood in terms of a long-range checkerboard alternation of JT axes in the monoclinic ac plane, which are coaligned on stacking along the b axis (Fig. 6). Melting of the orbital order has been reported for all RMn_7O_{12} except R = Pr, Nd, and Dy, as evidenced by a first order phase transition to the $Im\bar{3}$ aristotype occurring in the range 630–665 K at ambient pressure,[51,62,64,67] and under hydrostatic pressures greater than 34 GPa at RT (in $LaMn_7O_{12}$).[61] This $Im\bar{3}$ phase appears to be ubiquitous to the AMn_7O_{12} materials (Fig. 2), and we anticipate its discovery in the R = Pr, Nd, and Dy compounds should HT diffraction measurements be made. The orbitally ordered $I2/m$ crystal structure has been found to persist down to the lowest measured temperatures with the exception of YMn_7O_{12}, in which a $P2_1/n$ ground state was found to accompany the disordered yttrium dipolar glass.[67] Ferroelectric ground states have recently been proposed for compounds with R = La and Y, which would imply non-centrosymmetric structures at LT.[60,68]

The RMn_7O_{12} family of quadruple perovskite manganites have been considered in the context of functional material properties such as catalysis,[7,56,57] however most studies have focused on the microscopic cross-coupling of dipolar, orbital and magnetic degrees of freedom. Hence, it is this latter topic that we will focus on in the remainder of this section.
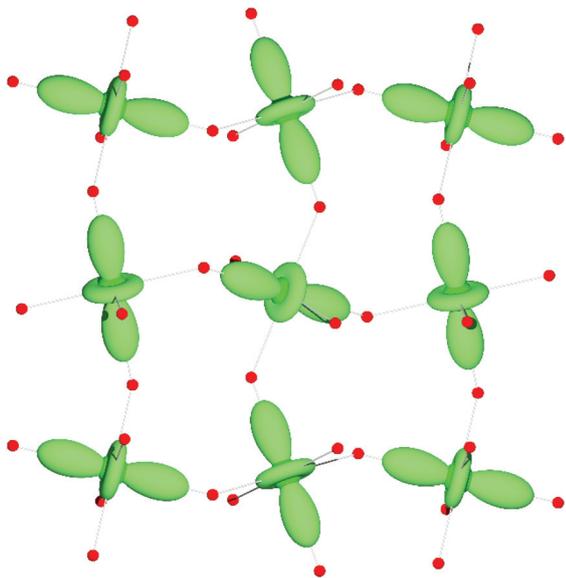
Fig. 6 LaMnO$_3$-type orbital order spanning the B site Mn^{3+} ions in any given *ac*-plane in monoclinic R^{3+}Mn$_7$O$_{12}$. The orbital order is co-aligned on moving along *b* (perpendicular to this figure) from one layer to the next.

CeMn$_7$O$_{12}$, SmMn$_7$O$_{12}$ and EuMn$_7$O$_{12}$ undergo a single magnetic phase transition at T_{N1} = 80, 87 and 87 K, respectively.[59,62,64] Both A′ and B site Mn^{3+} magnetic moments adopt long range order below T_{N1} with propagation vector $\boldsymbol{k}$ = (0, 0, 0). The A′-sites form a collinear ferrimagnetic structure, with magnetic moments lying in the *ac* plane and rotated away from the *c*-axis towards −*a* by 38.7(3)°, 34.7(4)°, and 32.1(5)° for R = Ce, Sm and Eu, respectively.[59] One in every three A′ site moments is uncompensated, giving a net ferrimagnetic moment as observed in magnetometry measurements. The B site Mn^{3+} magnetic moments form a C-type AFM structure (following the notation of Bertaut),[70] in which nearest neighbour moments are antiferromagnetically aligned in the *ac* plane, and coupled ferromagnetically along the *b* axis. B site spin canting is allowed by symmetry but could not be detected in

neutron powder diffraction experiments. Hence, a minimal model with B site moments collinear with the A′ site moments was proposed (Fig. 7).[59] Importantly, the magnetic structures on both sublattices transform by the same irreducible representation (Γ_2^+, defined w.r.t. the *I*2/*m* paramagnetic parent), hence the two are directly coupled and can develop together below a single phase transition. Based upon the Goodenough–Kanamori–Anderson rules[3] taken in the limit of 180° Mn–O–Mn bonds, the LaMnO$_3$ type orbital order should stabilise an A-type magnetic structure on the B sites (FM layers stacked AFM). This magnetic structure was indeed observed in LaMnO$_3$,[71] but it is the exact opposite of what is found in the above RMn$_7$O$_{12}$ compounds. The octahedral tilting in RMn$_7$O$_{12}$ is large compared to that of the RMnO$_3$ perovskites, leading to a more significant departure from 180° Mn–O–Mn bonds that may weaken or even change the sign of the superexchange interaction. In addition, the RMn$_7$O$_{12}$ compounds host strong d–d superexchange between A′ and B sublattices. Such A′–B exchange may compete with B–B exchange and play a key role in stabilising the C-type structure. We note that a B site A-type structure transforms by a different $\boldsymbol{k}$ = (0, 1, 0) irreducible representation to the observed $\boldsymbol{k}$ = (0, 0, 0) C-type structure, hence the energy gain through A′–B interactions would average to zero in this case.

Magnetic susceptibility and heat capacity measurements of GdMn$_7$O$_{12}$ and TbMn$_7$O$_{12}$ show anomalous behaviour at T_{N1} = 86 and 82 K, respectively, qualitatively similar to the behaviour of the R = Ce, Sm and Eu samples; hence consistent with a phase transition to the same ferrimagnetic ground state.[64] However, the microscopic nature of the long range magnetic order is yet to be confirmed, for example, by neutron powder diffraction experiments. Measurements of the isothermal magnetisation at 5 K indicate a sizeable uncompensated ferrimagnetic moment in both GdMn$_7$O$_{12}$ and TbMn$_7$O$_{12}$, which is enhanced compared to the R = Ce, Sm and Eu compounds likely due to the large moments carried by Gd and Tb. For all five samples discussed above, no direct evidence has been provided for long-range magnetic order of the rare-earth ions. However, a Schottky-like anomaly was observed in the specific
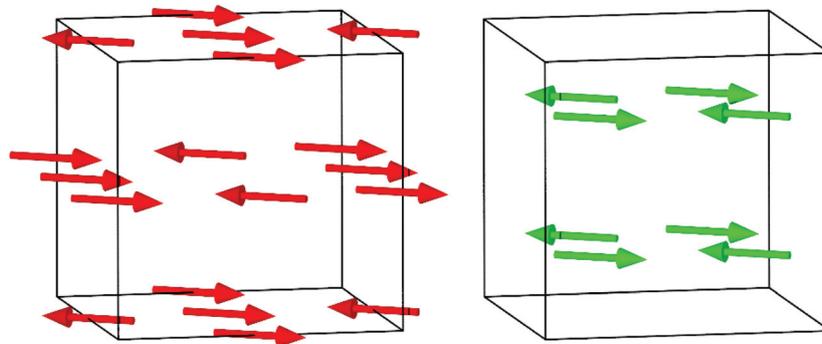

Fig. 7 The A′ site ferrimagnetic structure (red, left) and B site C-type antiferromagnetic structure (green, right) observed for R = La, Ce, Nd, Sm, Eu, Dy and Y, and likely common to all R^{3+}Mn$_7$O$_{12}$ compounds below T_{N1}.[59,65,67] The cubes represent the unit cell. The monoclinic *b*-axis points up the page, and the *c*-axis to the right.

heat of GdMn$_7$O$_{12}$ below ~10 K that was largely suppressed by a 9 T magnetic field.[64] This result may point towards Gd ions playing a significant role in the ground state. In addition, magnetic and specific heat measurements gave evidence that a second LT magnetic transition could emerge under magnetic fields in R = Sm and Eu.[64]

The dielectric constant of the R = Ce, Sm, Eu, Gd and Tb compounds has been reported,[62,64] measured as a function of both temperature and excitation frequency. In all cases a small kink-like anomaly was observed at T_{N1}, with the LT behaviour (frequency-dependent sharp steps between 18 and 35 K) otherwise dominated by extrinsic relaxation processes typical of these and related material systems. As such, there exists no evidence for dipolar or ferroelectric properties in these five compounds. N.B. Sharp steps in dielectric constant near 30 K were also reported in LaMn$_7$O$_{12}$, discussed below.[60]

PrMn$_7$O$_{12}$ is the only member of the RMn$_7$O$_{12}$ family that has two polymorphs at RT.[63] The $I2/m$ phase supports the same orbital order and ferrimagnetic magnetization below a single phase transition (T_{N1} = 70 K) as is characteristic of the compounds with R = Ce, Sm, Eu, Gd and Tb. Again, one might therefore speculate that the $I2/m$ polymorph of PrMn$_7$O$_{12}$ adopts the same ferrimagnetic structure below T_{N1}, but this is yet to be confirmed. The $R\bar{3}$ polymorph was reported to have the same crystal structure as CaMn$_7$O$_{12}$, implying a 3 : 1 splitting of B sites. In CaMn$_7$O$_{12}$ this splitting can be understood in terms of a 3 : 1 charge ordering of Mn^{3+} and Mn^{4+} ions from an average valence of Mn$^{3.25+}$ imposed by the divalent Ca cation. It is therefore somewhat surprising to find this polymorph in the RMn$_7$O$_{12}$ family (Fig. 2). Nonetheless, this $R\bar{3}$ phase displays altogether different magnetic behaviour with T_{N1} = 44 K,[63] and it has been proposed that in the $R\bar{3}$ symmetry the B-site Mn^{3+} ions split into three high spin and one low spin per formula unit, with the low spin ion at the undistorted octahedral site occupied by Mn^{4+} in CaMn$_7$O$_{12}$.

LaMn$_7$O$_{12}$ is arguably the most studied of all RMn$_7$O$_{12}$ compounds. Unlike the above, LaMn$_7$O$_{12}$ displays two magnetic phase transitions at T_{N1} = 79.5 and T_{N2} = 22.5 K.[52] The HT transition was first assigned to the onset of the same B site C-type AFM structure described above, but independent of A′ site Mn order which was instead assigned to the LT transition – an observation akin to the behaviour of NaMn$_7$O$_{12}$.[12] The proposed LT A′ site order had propagation vector $\boldsymbol{k}$ = (0, 1, 0), with FM layers in the ac plane, stacked AFM along b. Owing to the different symmetries, the A′ sites could naturally order independently of the B sites. Both A′ and B sublattice magnetic structures refined against neutron powder diffraction experiments[52] did not have a net ferrimagnetic moment – a result inconsistent with magnetometry measurements showing a net magnetisation similar to that measured for R = Ce, Pr, Sm, Eu, Gd and Tb. It was therefore proposed that the net moment in LaMn$_7$O$_{12}$ arose through an exceptionally large canting of the B site magnetic structure induced by the Dzyaloshinskii–Moriya interaction.[52] The application of the same model to YMn$_7$O$_{12}$ led to the suggestion that the A′ Mn sublattice remains disordered as only one magnetic transition was

found.[66] More recently, analysis of high resolution neutron powder diffraction data has shown that both A′ and B Mn moments order together at the HT transition with the same magnetic structure found for R = Ce, Sm and Eu, hence providing a more natural explanation for the sizeable ferrimagnetic moment.[59] We note that these two different scenarios manifest in remarkably subtle changes in the neutron powder diffraction pattern.[59] The latter scenario requires a more complex explanation for the LT transition, and it was proposed that LaMn$_7$O$_{12}$ enters into a ground state in which B site moments adopt a canted magnetic structure characterised by an admixture of commensurate C-type and A-type modes.[59] Intriguingly, such a ground state points towards an underlying instability towards the A-type structure expected in the presence of LaMnO$_3$-type orbital order – perhaps acting in competition A′–B superexchange.

NdMn$_7$O$_{12}$ was found to undergo three magnetic phase transitions, one at T_{N1} = 85 K, and a further two at low temperature (T_{N2} = 12 and T_{N3} = 8.5 K). Both A′ and B sublattices were found to order below T_{N1} with ferrimagnetic and C-type magnetic structures, respectively – in common with all of the above RMn$_7$O$_{12}$ compounds.[59] It was reported that below the second transition there developed an incommensurate modulation of the B-site magnetic structure with $\boldsymbol{k}$ = (0.248(2), 1, 0.064(3)), which corresponds to an admixture of commensurate C-type and incommensurate A-type modes. In comparison with LaMn$_7$O$_{12}$, the incommensurate modulation of NdMn$_7$O$_{12}$ can be thought of as a spatially varying unidirectional canting (addition of an orthogonal spin density wave) or as a conical rotation of moments (addition of an orthogonal cycloid). These two scenarios could not be differentiated by neutron powder diffraction, but both support the argument for competing magnetic instabilities in both R = La and Nd compounds (it is well established that incommensurate structures can be stabilised by competing interactions). Below the third transition the incommensurate propagation vector was found to jump to $\boldsymbol{k}$ = (0.3231(7), 1, 0.0069(7)), accompanied by a finite ordered moment appearing on the Nd ions.

It is apparent that the additional LT magnetic transitions occur for compounds with rare earth ions of largest ionic radii, with the exceptions of CeMn$_7$O$_{12}$ and PrMn$_7$O$_{12}$. It was suggested that this discrepancy may arise due to Ce$_{1-x}$Mn$_{7+x}$O$_{12}$ or PrMn$_7$O$_{12+d}$ off-stoichiometry of the measured samples. Indeed, the second transition was found to be suppressed in non-stoichiometric La$_{0.9}$Mn$_{7.1}$O$_{12}$.[59,62] The experimental results published to date indicate complex behaviour at low temperatures, and we suggest future studies, both experimental and theoretical, are required to establish the full microscopic details of the ground state magnetic structures of LaMn$_7$O$_{12}$ and NdMn$_7$O$_{12}$, and the underlying competing interactions in the RMn$_7$O$_{12}$ family.

Unpublished dielectric measurements of LaMn$_7$O$_{12}$ and NdMn$_7$O$_{12}$ indicate qualitatively similar behaviour to the non-polar compounds with R = Ce, Sm, Eu, Gd and Tb. Recently, however, a large electric polarisation of up to 0.56 μC cm^{-2} has

been suggested for $LaMn_7O_{12}$ developing below T_{N1},[60] based on the observation of very strong, broad and symmetrical pyro-electric-current peaks. Following the reported giant ferroelectric polarisation in $CaMn_7O_{12}$ (ref. 41) some debate ensued regarding the intrinsic nature of the polarisation in these systems. Indeed, other works have assigned such pyroelectric-current peaks to extrinsic effects.[44,48,62,64] In light of this, we suggest that it is important for extrinsic effects, for example those due to thermally stimulated currents, to be ruled out in the case of $LaMn_7O_{12}$.

Specific heat and magnetometry measurements showed that YMn_7O_{12} supports a single ferrimagnetic phase transition at T_{N1} = 108 K;[66] approximately 20–30 K higher than the RMn_7O_{12} compounds discussed above. Unlike the other RMn_7O_{12} compounds, YMn_7O_{12} was found to undergo a structural phase transition at T_s = 200 K that was clearly marked by anomalous behaviour in the temperature dependence of the specific heat and spontaneous negative thermal expansion of the lattice.[66] The microscopic details of both phase transitions were established in a later publication, in which the same ferrimagnetic structure discussed above was reported to occur below T_{N1}, apparently independent of the structural transition at T_s.[67] The ground state crystal structure was characterised by an ordered pattern of atomic displacements that lowered the crystal symmetry to $P2_1/n$, accompanied by disordered displacements of yttrium ions forming a so-called dipolar glass that naturally explained the observed negative thermal expansion.[67] A recent publication based on single crystal diffraction measurements showed that the yttrium ions can form partial antiferroelectric order out of the dipolar glass state,[68] the extent of which is likely sample dependent. The structural modifications below T_s could in principle occur independent of one another, but they all improve the bonding conditions of the yttrium ions that were shown to be somewhat underbonded above T_s.[67] Hence, YMn_7O_{12} has a *pseudo*-JT instability associated with A site cations – phenomena usually associated with B site cations in perovskite-derived materials – that can drive unusual LT structural phase transitions. We note that, compared to the $RMnO_3$ systems, the quadruple perovskites may be prone to underbonding of R cations as the octahedral tilts primarily generate square planar coordinations for the majority A′ site Mn^{3+} ions, perhaps at the expense of the minority A site R ions. Pyroelectric current measurements similar to those reported for $LaMn_7O_{12}$ have also led to the suggestion of a large ferroelectric polarisation developing in YMn_7O_{12} at low temperature.[68] As before, we stress a similar level of caution when interpreting the results of these measurements.

Finally, the reported phenomenology of $DyMn_7O_{12}$ is similar to that of YMn_7O_{12} but with one key difference; the structural and magnetic transitions come together (T_{N1} and T_s are merged) to create a single, first order magneto-structural phase transition at T_{N1} ~95 K.[65] Below T_{N1} the Dy dipolar glass and ferrimagnetic order parameters were found to be cross-coupled (note that in $DyMn_7O_{12}$ ordered atomic displacements were not observed below T_{N1}),[65] as demonstrated by temperature and field dependent dielectric constant measurements

(Fig. 8) (N.B. when T_{N1} and T_s are separated as in YMn_7O_{12} no dielectric anomalies were found at the both temperatures).[65] In addition, long-range FM ordering of Dy magnetic moments was found below 5.5 K.[65]

In summary, all RMn_7O_{12} compounds host a common magnetic structure composed of a ferrimagnetic A′ site Mn^{3+} sublattice with one uncompensated Mn^{3+} moment per unit cell, and a C-type AFM B site sublattice (Fig. 7). In addition, $LaMn_7O_{12}$ and $NdMn_7O_{12}$ show LT magnetic phase transitions likely associated with the competition between A′–B and B–B exchange. For compounds with small R ionic radius (R = Dy and Y), the R cations adopt a *pseudo*-JT instability that leads to exotic LT phases characterised by cross-coupled magnetic and electric degrees of freedom.

5. $BiMn_7O_{12}$

Compared with RMn_7O_{12}, $BiMn_7O_{12}$ has an electronic instability originating from the presence of the lone-electron pair of Bi^{3+} cations. As a result, it exhibits distinct structural, magnetic and dielectric properties. $BiMn_7O_{12}$ was first reported in 2008,[72] and its RT crystal structure was often described using a centrosymmetric $I2/m$ model derived from powder diffraction experiments.[53,58,73,74] On the other hand, more sensitive single-crystal structural investigations gave evidence for polar Im symmetry at RT.[58,75] A number of additional structural phase transitions were later found,[58,76] and the sequence of phase transitions is now well established (on cooling) as $Im\bar{3} \Rightarrow I2/m \Rightarrow [R\bar{1}(\alpha\beta\gamma)0] \Rightarrow Im \Rightarrow I1$ with transitions at about 608 K, 460 K, and 295 K, respectively, where $[R\bar{1}(\alpha\beta\gamma)0]$ denotes an incipient phase, which appears only as diffuse scattering in undoped $BiMn_7O_{12}$ between the $I2/m$ and Im phases.[58] The proper stabilisation of the $R\bar{1}(\alpha\beta\gamma)0$ phase can be triggered by small Cu^{2+} or Fe^{3+} doping.[35] The $Im\bar{3} \Rightarrow I2/m$ transition is related to orbital ordering of Mn^{3+} similar to RMn_7O_{12}, and the $I2/m \Rightarrow Im$ transition – to the development of a ferroelectric polarization associated with the Bi^{3+} lone pair electrons. However, no direct confirmation of ferroelectricity (such as P–E loops) has been obtained to date.

Two magnetic transitions were widely reported in $BiMn_7O_{12}$ at about T_{N1} = 59 K and T_{N2} = 21 K in analogy with $LaMn_7O_{12}$,[72,74,75,77] despite the first paper (ref. 72) reporting evidence for three magnetic transitions from specific heat measurements. In comparison with RMn_7O_{12}, frequency-independent peaks in the dielectric constant of $BiMn_7O_{12}$ were observed at all (three) magnetic transition temperatures without any extrinsic steps,[72,75,78] but no pyroelectric current anomalies have been detected. Therefore, the origin of dielectric peaks remains unclear and needs further investigation.

The only neutron diffraction study of the magnetic structures assumed that Mn at the B sites are ordered at T_{N1}, and Mn at the A′ sites are ordered at T_{N2}, in analogy with $LaMn_7O_{12}$.[74] In addition, the total zero moment was assumed for both A′ and B sites despite the observation of large uncompensated moments on M versus H curves (*e.g.*, about $1\mu_B$ at 2 K
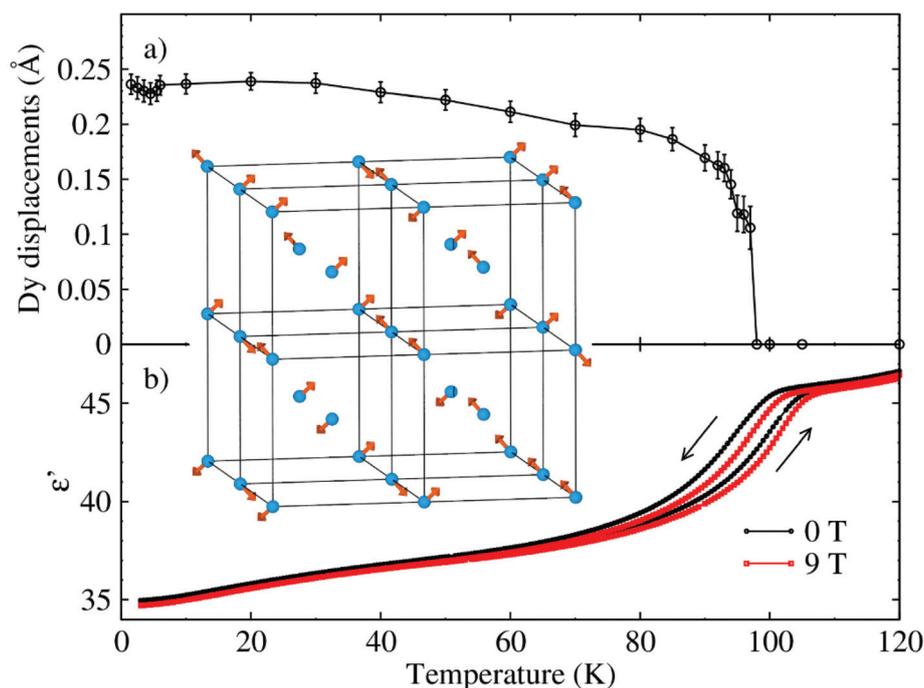
Fig. 8 The magnetostructural dipolar glass found in $(Dy_{0.91}Mn_{0.09})Mn_7O_{12}$: (a) The temperature dependence of the disordered Dy atomic displacement amplitudes established through structural refinements against neutron powder diffraction data,[65] and (b) the temperature dependence of the real dielectric constant measured in 0 T (black) and 9 T (red) applied magnetic fields.[65] The inset illustrates the disordered Dy dipolar glass (circles are ideal positions of Dy atoms at the (0,0,0) site; arrows show displacements).

and $0.8\mu_B$ at 40 K).[72,77] Furthermore, in the analysis of the magnetic structures the (crystal) symmetry was considered to be Im,[74] while the real ground-state symmetry is $I1$. Hence, we suggest that the magnetic structures of $BiMn_7O_{12}$ need careful re-investigation.

Similar to $PrMn_7O_{12}$, several modifications of $BiMn_7O_{12}$ were reported at RT (monoclinic, rhombohedral and cubic).[73,77–79] However, in this case, the polymorphism was assigned to cation non-stoichiometry $(Bi_{1-x/3}(Mn^{3+}_3)(Mn^{3+}_{4-x}Mn^{4+}_x)O_{12}$ and $Bi_{0.94}Mn_{6.91}O_{12})$ and the appearance of Mn^{4+} at the B sites. We believe the same should be true for $PrMn_7O_{12}$. Magnetic properties of non-stoichiometric $BiMn_7O_{12}$ were noticeably different from stoichiometric $BiMn_7O_{12}$.

6. Conclusions

We have reviewed the current state of research on AMn_7O_{12} quadruple perovskite manganites and identified some future directions, such as the re-investigation of magnetic structures of $NaMn_7O_{12}$ and $BiMn_7O_{12}$ and understanding dielectric behavior of all members, in particular, $BiMn_7O_{12}$. Investigations of different solid solutions[35,80–82] may also yield fascinating results, as it allows continuous variations of Mn oxidation states at the B sites, while keeping nearly the same B-site Mn–O–Mn bond angles,[82] as was extensively studied in the mixed-valence $R_{1-x}A_xMnO_3$ perovskites.

Conflicts of interest

There are no conflicts to declare.

Acknowledgements

References

1 J. M. D. Coey, M. Viret and S. von Molnar, Mixed-valence manganites, *Adv. Phys.*, 2009, **58**, 571–697.
2 C. Zener, Interaction between the d-shells in the transition metals. II. Ferromagnetic compounds of manganese with perovskite structure, *Phys. Rev.*, 1951, **82**, 403–405.
3 J. B. Goodenough, Theory of the role of covalence in the perovskite-type manganites [La,M(II)]MnO$_3$, *Phys. Rev.*, 1955, **100**, 564–573.
4 S. Jin, T. H. Tiefel, M. McCormack, R. A. Fastnacht, R. Ramesh and L. H. Chen, Thousandfold change in resis-

tivity in magnetoresistive La-Ca-Mn-O films, *Science*, 1994, **264**, 413–415.

5 E. Dagotto, T. Hotta and A. Moreo, Colossal magnetoresistant materials: the key role of phase separation, *Phys. Rep.*, 2001, **344**, 1–153.

6 T. Kimura, T. Goto, H. Shintani, K. Ishizaka, T. Arima and Y. Tokura, Magnetic control of ferroelectric polarization, *Nature*, 2003, **426**, 55–58.

7 I. Yamada, H. Fujii, A. Takamatsu, H. Ikeno, K. Wada, H. Tsukasaki, S. Kawaguchi, S. Mori and S. Yagi, Bifunctional oxygen reaction catalysis of quadruple manganese perovskites, *Adv. Mater.*, 2017, **29**, 1603004.

8 A. N. Vasil'ev and O. S. Volkova, New functional materials $AC_3B_4O_{12}$ (review), *Low Temp. Phys.*, 2007, **33**, 895–914.

9 A. M. Glazer, The classification of tilted octahedra in perovskites, *Acta Crystallogr., Sect. B: Struct. Crystallogr. Cryst. Chem.*, 1972, **28**, 3384–3392.

10 M. Marezio, P. D. Dernier, J. Chenavas and J. C. Joubert, High pressure synthesis and crystal structure of $NaMn_7O_{12}$, *J. Solid State Chem.*, 1973, **6**, 16–20.

11 J. Chenavas, F. Sayetat, A. Collomb, J. C. Joubert and M. Marezio, X-ray study of the low-temperature phase of $[NaMn^{3+}_3](Mn^{3+}_2Mn^{4+}_2)O_{12}$, a perovskite-like compound, *Solid State Commun.*, 1975, **16**, 1129–1132.

12 A. Prodi, E. Gilioli, A. Gauzzi, F. Licci, M. Marezio, F. Bolzoni, Q. Huang, A. Santoro and J. W. Lynn, Charge orbital and spin ordering phenomena in the mixed valence manganite $(NaMn^{3+}_3)(Mn^{3+}_2Mn^{4+}_2)O_{12}$, *Nat. Mater.*, 2004, **3**, 48–52.

13 S. V. Streltsov and D. I. Khomskii, Jahn-Teller distortion and charge, orbital, and magnetic order in $NaMn_7O_{12}$, *Phys. Rev. B: Condens. Matter Mater. Phys.*, 2014, **89**, 201115.

14 A. Prodi, A. Daoud-Aladine, F. Gozzo, B. Schmitt, O. Lebedev, G. van Tendeloo, E. Gilioli, F. Bolzoni, H. Aruga-Katori, H. Takagi, M. Marezio and A. Gauzzi, Commensurate structural modulation in the charge- and orbitally ordered phase of the quadruple perovskite $(NaMn_3)Mn_4O_{12}$, *Phys. Rev. B: Condens. Matter Mater. Phys.*, 2014, **90**, 180101.

15 V. P. Gastaldo, Y. Klein, B. Baptiste, R. Cabassi, E. Gilioli, A. Gauzzi and A. J. A. de Oliveira, Unconventional magnetic ferroelectricity in the quadruple perovskite $NaMn_7O_{12}$, *Phys. Rev. B: Condens. Matter Mater. Phys.*, 2020, **102**, 161120.

16 E. Gilioli, G. Calestani, F. Licci, A. Gauzzi, F. Bolzoni, A. Prodi and M. Marezio, P–T phase diagram and single crystal structural refinement of $NaMn_7O_{12}$, *Solid State Sci.*, 2005, **7**, 746–752.

17 R. Cabassi, F. Bolzoni, A. Gauzzi, E. Gilioli, A. Prodi and F. Licci, Dielectric properties of doping-free $NaMn_7O_{12}$: Origin of the observed colossal dielectric constant, *Phys. Rev. B: Condens. Matter Mater. Phys.*, 2006, **74**, 045212.

18 E. Gilioli, G. Calestani, F. Licci, C. Paorici, A. Gauzzi, F. Bolzoni and A. Prodi, High-pressure growth of $NaMn_7O_{12}$ crystals, *J. Solid State Chem.*, 2006, **179**, 3839–3848.

19 D. Delmonte, F. Mezzadri, F. Orlandi, G. Calestani, Y. Amiel and E. Gilioli, High pressure induced insulator-to-semimetal transition through intersite charge transfer in $NaMn_7O_{12}$, *Crystals*, 2018, **8**, 81.

20 B. Bochu, J. Chenavas, J. C. Joubert and M. Marezio, High pressure synthesis and crystal structure of a new series of perovskite-like compounds CMn_7O_{12} (C = Na, Ca, Cd, Sr, La, Nd), *J. Solid State Chem.*, 1974, **11**, 88–93.

21 H. S. Horowitz and J. M. Longo, Phase relations in the Ca-Mn-O system, *Mater. Res. Bull.*, 1978, **13**, 1559–1369.

22 B. Bochu, J. L. Buevoz, J. Chenavas, A. Collomb, J. C. Joubert and M. Marezio, Bond lengths in $[CaMn_3](Mn_4)O_{12}$: A new Jahn–Teller distortion of Mn^{3+} octahedral, *Solid State Commun.*, 1980, **36**, 133–138.

23 D. Khomskii and J. van den Brink, Anharmonic effects on charge and orbital order, *Phys. Rev. Lett.*, 2000, **85**, 3329.

24 R. Przeniosło, I. Sosnowska, E. Suard, A. Hewat and A. N. Fitch, Phase coexistence in the charge ordering transition in $CaMn_7O_{12}$, *J. Phys.: Condens. Matter*, 2002, **14**, 5747–5753.

25 W. Sławiński, R. Przeniosło, I. Sosnowska, M. Bieringer, I. Margiolaki, A. N. Fitch and E. Suard, Charge ordering in $CaCu_xMn_{7-x}O_{12}$ (x = 0.0 and 0.1) compounds, *J. Phys.: Condens. Matter*, 2008, **20**, 104239.

26 W. Sławiński, R. Przeniosło, I. Sosnowska and M. Bieringer, Structural and magnetic modulations in $CaCu_xMn_{7-x}O_{12}$, *J. Phys.: Condens. Matter*, 2010, **22**, 186001.

27 W. Sławiński, R. Przeniosło, I. Sosnowska, M. Bieringer, I. Margiolakic and E. Suard, Modulation of atomic positions in $CaCu_xMn_{7-x}O_{12}$ ($x \leq 0.1$), *Acta Crystallogr., Sect. B: Struct. Sci.*, 2009, **65**, 535–542.

28 W. Sławiński, R. Przeniosło, I. Sosnowska and V. Petříček, Helical screw type magnetic structure of the multiferroic $CaMn_7O_{12}$ with low Cu-doping, *Acta Crystallogr., Sect. B: Struct. Sci.*, 2012, **68**, 240–249.

29 A. A. Belik, Y. S. Glazkova, Y. Katsuya, M. Tanaka, A. V. Sobolev and I. A. Presniakov, Low-temperature structural modulations in $CdMn_7O_{12}$, $CaMn_7O_{12}$, $SrMn_7O_{12}$, and $PbMn_7O_{12}$ perovskites studied by synchrotron X-ray powder diffraction and Mössbauer spectroscopy, *J. Phys. Chem. C*, 2016, **120**, 8278–8288.

30 N. J. Perks, R. D. Johnson, C. Martin, L. C. Chapon and P. G. Radaelli, Magneto-orbital helices as a route to coupling magnetism and ferroelectricity in multiferroic $CaMn_7O_{12}$, *Nat. Commun.*, 2012, **3**, 1277.

31 R. D. Johnson, D. D. Khalyavin, P. Manuel, P. G. Radaelli, I. S. Glazkova, N. Terada and A. A. Belik, Magneto-orbital ordering in the divalent A-site quadruple perovskite manganites AMn_7O_{12} (A = Sr, Cd, and Pb), *Phys. Rev. B: Condens. Matter Mater. Phys.*, 2017, **96**, 054448.

32 H. Guo, M. T. Fernández-Daz, L. Zhou, Y. Yin, Y. Long and A. C. Komarek, Non-collinear magnetic structure of manganese quadruple perovskite $CdMn_7O_{12}$, *Sci. Rep.*, 2017, **7**, 45939.

33 Y. S. Glazkova, N. Terada, Y. Matsushita, Y. Katsuya, M. Tanaka, A. V. Sobolev, I. A. Presniakov and A. A. Belik, High-pressure synthesis, crystal structures, and properties of $CdMn_7O_{12}$ and $SrMn_7O_{12}$ perovskites, *Inorg. Chem.*, 2015, **54**, 9081–9091.

34 R. D. Johnson, D. D. Khalyavin, P. Manuel and A. A. Belik, Competing electronic instabilities in the quadruple perovskite manganite $PbMn_7O_{12}$, *Phys. Rev. B: Condens. Matter Mater. Phys.*, 2021, **103**, 134115.

35 D. D. Khalyavin, R. D. Johnson, F. Orlandi, P. G. Radaelli, P. Manuel and A. A. Belik, Emergent helical texture of electric dipoles, *Science*, 2020, **369**, 680–684.

36 T. Locherer, R. Dinnebier, R. K. Kremer, M. Greenblatt and M. Jansen, Synthesis and properties of a new quadruple perovskite: A-site-ordered $PbMn_3Mn_4O_{12}$, *J. Solid State Chem.*, 2012, **190**, 277–284.

37 S. V. Ovsyannikov, A. M. Abakumov, A. A. Tsirlin, W. Schnelle, R. Egoavil, J. Verbeeck, G. Van Tendeloo, K. V. Glazyrin, M. Hanfland and L. Dubrovinsky, Perovskite-like Mn_2O_3: a path to new manganites, *Angew. Chem., Int. Ed.*, 2013, **52**, 1494–1498.

38 D. D. Khalyavin, R. D. Johnson, P. Manuel, A. A. Tsirlin, A. M. Abakumov, D. P. Kozlenko, Y. Sun, L. Dubrovinsky and S. V. Ovsyannikov, Magneto-orbital texture in the perovskite modification of Mn_2O_3, *Phys. Rev. B: Condens. Matter Mater. Phys.*, 2018, **98**, 014426.

39 W. T. Chen, C. W. Wang, H. C. Wu, F. C. Chou, H. D. Yang, A. Simonov and M. S. Senn, Improper ferroelectric polarization in a perovskite driven by intersite charge transfer and ordering, *Phys. Rev. B: Condens. Matter Mater. Phys.*, 2018, **97**, 144102.

40 A. A. Belik, Y. Matsushita and D. D. Khalyavin, Reentrant structural transitions and collapse of charge and orbital orders in quadruple perovskites, *Angew. Chem., Int. Ed.*, 2017, **56**, 10423–10427.

41 R. D. Johnson, L. C. Chapon, D. D. Khalyavin, P. Manuel, P. G. Radaelli and C. Martin, Giant improper ferroelectricity in the ferroaxial magnet $CaMn_7O_{12}$, *Phys. Rev. Lett.*, 2012, **108**, 067201.

42 G. Zhang, S. Dong, Z. Yan, Y. Guo, Q. Zhang, S. Yunoki, E. Dagotto and J.-M. Liu, Multiferroic properties of $CaMn_7O_{12}$, *Phys. Rev. B: Condens. Matter Mater. Phys.*, 2011, **84**, 174413.

43 R. D. Johnson, D. D. Khalyavin, P. Manuel, A. Bombardi, C. Martin, L. C. Chapon and P. G. Radaelli, Modulated spin helicity stabilized by incommensurate orbital density waves in a quadruple perovskite manganite, *Phys. Rev. B: Condens. Matter Mater. Phys.*, 2016, **93**, 180403(R).

44 N. Terada, Y. S. Glazkova and A. A. Belik, Differentiation between ferroelectricity and thermally stimulated current in pyrocurrent measurements of multiferroic MMn_7O_{12} (M = Ca, Sr, Cd, Pb), *Phys. Rev. B: Condens. Matter Mater. Phys.*, 2016, **93**, 155127.

45 R. D. Johnson, S. Nair, L. C. Chapon, A. Bombardi, C. Vecchini, D. Prabhakaran, A. T. Boothroyd and P. G. Radaelli, $Cu_3Nb_2O_8$: a multiferroic with chiral coupling to the crystal structure, *Phys. Rev. Lett.*, 2011, **107**, 137205.

46 S. W. Cheong and M. Mostovoy, Multiferroics: a magnetic twist for ferroelectricity, *Nat. Mater.*, 2007, **6**, 13–20.

47 J. Cong, K. Zhai, Y. Chai, D. Shang, D. D. Khalyavin, R. D. Johnson, D. P. Kozlenko, S. E. Kichanov, A. M. Abakumov, A. A. Tsirlin, L. Dubrovinsky, X. Xu, Z. Sheng, S. V. Ovsyannikov and Y. Sun, Spin-induced multiferroicity in the binary perovskite manganite Mn_2O_3, *Nat. Commun.*, 2018, **9**, 2996.

48 A. A. Belik, Y. S. Glazkova, N. Terada, Y. Matsushita, A. V. Sobolev, I. A. Presniakov, N. Tsujii, S. Nimori, K. Takehana and Y. Imanaka, Spin-driven multiferroic properties of $PbMn_7O_{12}$ perovskite, *Inorg. Chem.*, 2016, **55**, 6169–6177.

49 K. Gautam, S. S. Majid, S. Francoual, A. Ahad, K. Dey, M. C. Rahn, R. Sankar, F. C. Chou and D. K. Shukla, Magnetic and orbital correlations in multiferroic $CaMn_7O_{12}$ probed by X-ray resonant elastic scattering, *Phys. Rev. B: Condens. Matter Mater. Phys.*, 2020, **101**, 224430.

50 A. Prodi, G. Allodi, E. Gilioli, F. Licci, M. Marezio, F. Bolzoni, A. Gauzzi and R. De Renzi, μSR study of $AA'_3Mn_4O_{12}$ double perovskites, *Phys. B*, 2006, **374–375**, 55–58.

51 H. Okamoto, M. Karppinen, H. Yamauchi and H. Fjellvag, High-temperature synchrotron X-ray diffraction study of $LaMn_7O_{12}$, *Solid State Sci.*, 2009, **11**, 1211–1215.

52 A. Prodi, E. Gilioli, R. Cabassi, F. Bolzoni, F. Licci, Q. Huang, J. W. Lynn, M. Affronte, A. Gauzzi and M. Marezio, Magnetic structure of the high-density single-valent eg Jahn-Teller system $LaMn_7O_{12}$, *Phys. Rev. B: Condens. Matter Mater. Phys.*, 2009, **79**, 085105.

53 H. Okamoto, N. Imamura, M. Karppinen, H. Yamauchi and H. Fjellvag, Square coordinated MnO_2-units in $BiMn_7O_{12}$, *Inorg. Chem.*, 2010, **49**, 8709–8712.

54 X. J. Liu, S. H. Lv, E. Pan, J. Meng and J. D. Albrecht, First-principles study of crystal structural stability and electronic and magnetic properties in $LaMn_7O_{12}$, *J. Phys.: Condens. Matter*, 2010, **22**, 246001.

55 R. Cabassi, F. Bolzoni, E. Gilioli, F. Bissoli, A. Prodi and A. Gauzzi, Jahn-Teller-induced crossover of the paramagnetic response in the singly valent eg system $LaMn_7O_{12}$, *Phys. Rev. B: Condens. Matter Mater. Phys.*, 2010, **81**, 214412.

56 I. Yamada, Novel catalytic properties of quadruple perovskites, *Sci. Technol. Adv. Mater.*, 2017, **18**, 541–548.

57 A. Takamatsu, I. Yamada, S. Yagi and H. Ikeno, Oxygen evolution via the bridging inequivalent dual-site reaction: first-principles study of a quadruple-perovskite oxide catalyst, *J. Phys. Chem. C*, 2017, **121**, 28403–28411.

58 A. A. Belik, Y. Matsushita, Y. Kumagai, Y. Katsuya, M. Tanaka, S. Yu. Stefanovich, B. I. Lazoryak, F. Oba and K. Yamaura, Complex structural behavior of $BiMn_7O_{12}$ quadruple perovskite, *Inorg. Chem.*, 2017, **56**, 12272–12281.

59 R. D. Johnson, D. D. Khalyavin, P. Manuel, L. Zhang, K. Yamaura and A. A. Belik, Magnetic structures of the rare-earth quadruple perovskite manganites RMn_7O_{12}, *Phys. Rev. B: Condens. Matter Mater. Phys.*, 2018, **98**, 104423.

60 A. Gauzzi, F. P. Milton, V. Pascotto Gastaldo, M. Verseils, A. J. Gualdi, D. von Dreifus, Y. Klein, D. Garcia, A. J. A. de Oliveira, P. Bordet and E. Gilioli, Ferroelectricity in the 1 μC cm^{-2} range induced by canted antiferromagnetism in $(LaMn_3)Mn_4O_{12}$, *Appl. Phys. Lett.*, 2019, **115**, 152902.

61 V. S. Bhadram, B. Joseph, D. Delmonte, E. Gilioli, B. Baptiste, Y. Le-Godec, R. P. S. M. Lobo and A. Gauzzi, Reentrant phase transition and suppression of Jahn-Teller distortion in the quadruple perovskite structure under high pressure, arXiv:2102.09998, 2021.

62 A. A. Belik, L. Zhang, N. Terada, Y. Katsuya, M. Tanaka, Y. Matsushita and K. Yamaura, A-site-ordered quadruple perovskite manganite $CeMn_7O_{12}$ with trivalent cations, *J. Solid State Chem.*, 2020, **283**, 121161.

63 F. Mezzadri, M. Calicchio, E. Gilioli, R. Cabassi, F. Bolzoni, G. Calestani and F. Bissoli, High-pressure synthesis and characterization of $PrMn_7O_{12}$ polymorphs, *Phys. Rev. B: Condens. Matter Mater. Phys.*, 2009, **79**, 014420.

64 L. Zhang, N. Terada, R. D. Johnson, D. D. Khalyavin, P. Manuel, Y. Katsuya, M. Tanaka, Y. Matsushita, K. Yamaura and A. A. Belik, High-pressure synthesis, structures, and properties of trivalent A-site-ordered quadruple perovskites RMn_7O_{12} (R = Sm, Eu, Gd, and Tb), *Inorg. Chem.*, 2018, **57**, 5987–5998.

65 R. D. Johnson, D. D. Khalyavin, P. Manuel, L. Zhang, K. Yamaura and A. A. Belik, Emergence of a magnetostructural dipolar glass in the quadruple perovskite $Dy_{1-\delta}Mn_{7+\delta}O_{12}$, *Phys. Rev. Lett.*, 2020, **125**, 097601.

66 M. Verseils, F. Mezzadri, D. Delmonte, B. Baptiste, Y. Klein, S. Shcheka, L. C. Chapon, T. Hansen, E. Gilioli and A. Gauzzi, Effect of chemical pressure induced by La^{3+}/Y^{3+} substitution on the magnetic ordering of $(AMn_3)Mn_4O_{12}$ quadruple perovskites, *Phys. Rev. Mater.*, 2017, **1**, 064407.

67 R. D. Johnson, D. D. Khalyavin, P. Manuel, Y. Katsuya, M. Tanaka, Y. Matsushita, L. Zhang, K. Yamaura and A. A. Belik, Displacive structural phase transitions and the magnetic ground state of quadruple perovskite YMn_7O_{12}, *Phys. Rev. B: Condens. Matter Mater. Phys.*, 2019, **99**, 024107.

68 M. Verseils, F. Mezzadri, D. Delmonte, R. Cabassi, B. Baptiste, Y. Klein, G. Calestani, F. Bolzoni, E. Gilioli and A. Gauzzi, Centrosymmetry breaking and ferroelectricity driven by short-range magnetic order in the quadruple perovskite $(YMn_3)Mn_4O_{12}$, *Inorg. Chem.*, 2019, **58**, 14204–14211.

69 J. Rodríguez-Carvajal, M. Hennion, F. Moussa, A. H. Moudden, L. Pinsard and A. Revcolevschi, Neutron-diffraction study of the Jahn-Teller transition in stoichiometric $LaMnO_3$, *Phys. Rev. B: Condens. Matter Mater. Phys.*, 1998, **57**, R3189–R3192.

70 E. F. Bertaut, *Magnetism*, ed. G. T. Rado and H. Suhl, Academic, New York, 1963, vol. 3, p. 149.

71 E. O. Wollan and W. C. Koehler, Neutron diffraction study of the magnetic properties of the series of perovskite-type compounds $[(1-x)La,xCa]MnO_3$, *Phys. Rev.*, 1955, **100**, 545–563.

72 N. Imamura, M. Karppinen, T. Motohashi, D. Fu, M. Itoh and H. Yamauchi, Positive and negative magnetodielectric effects in A-site ordered $(BiMn_3)Mn_4O_{12}$ perovskite, *J. Am. Chem. Soc.*, 2008, **130**, 14948–14949.

73 H. Okamoto, N. Imamura, M. Karppinen, H. Yamauchi and H. Fjellvag, Crystal structure of the monoclinic and cubic polymorphs of $BiMn_7O_{12}$, *J. Solid State Chem.*, 2010, **183**, 186–191.

74 A. Gauzzi, G. Rousse, F. Mezzadri, G. L. Calestani, G. Andre, F. Bouree, M. Calicchio, E. Gilioli, R. Cabassi, F. Bolzoni, A. Prodi, P. Bordet and M. Marezio, Magnetoelectric coupling driven by inverse magnetostriction in multiferroic $BiMn_3Mn_4O_{12}$, *J. Appl. Phys.*, 2013, **113**, 043920.

75 F. Mezzadri, G. Calestani, M. Calicchio, E. Gilioli, F. Bolzoni, R. Cabassi, M. Marezio and A. Migliori, Synthesis and characterization of multiferroic $BiMn_7O_{12}$, *Phys. Rev. B: Condens. Matter Mater. Phys.*, 2009, **79**, 100106.

76 W. A. Slawinski, H. Okamoto and H. Fjellvag, Triclinic crystal structure distortion of multiferroic $BiMn_7O_{12}$, *Acta Crystallogr., Sect. B: Struct. Sci., Cryst. Eng. Mater.*, 2017, **73**, 313–320.

77 N. Imamura, M. Karppinen and H. Yamauchi, Synthesis and properties of monoclinic and cubic forms of the A-site-ordered $(BiMn_3)Mn_4O_{12}$ perovskite, *Chem. Mater.*, 2009, **21**, 2179–2183.

78 F. Mezzadri, M. Buzzi, C. Pernechele, G. Calestani, M. Solzi, A. Migliori and E. Gilioli, Polymorphism and multiferroicity in $Bi_{1-x/3}(Mn^{III}_3)(Mn^{III}_{4-x}Mn^{IV}_x)O_{12}$, *Chem. Mater.*, 2011, **23**, 3628–3635.

79 N. Imamura, K. Singh, D. Pelloquin, C. Simon, T. Sasagawa, M. Karppinen, H. Yamauchi and A. Maignan, Magnetodielectric response of square-coordinated MnO_2 unit in cubic $BiMn_7O_{12}$, *Appl. Phys. Lett.*, 2011, **98**, 072903.

80 A. A. Belik, Y. Matsushita, M. Tanaka, R. D. Johnson and D. D. Khalyavin, A plethora of structural transitions, distortions and modulations in Cu-doped $BiMn_7O_{12}$ quadruple perovskites, *J. Mater. Chem. C*, 2021, **9**, 10232–10242.

81 R. D. Johnson, F. Mezzadri, P. Manuel, D. D. Khalyavin, E. Gilioli and P. G. Radaelli, Evolution of magneto-orbital order upon B-site electron doping in $Na_{1-x}Ca_xMn_7O_{12}$ quadruple perovskite manganites, *Phys. Rev. Lett.*, 2018, **120**, 257202.

82 W.-T. Chen, C.-W. Wang, C.-C. Cheng, Y.-C. Chuang, A. Simonov, N. C. Bristowe and M. S. Senn, Striping of orbital-order with charge-disorder in optimally doped manganites, arXiv:2104.14274, 2021.